First Observation of Superlattice Reflections in the Hidden Order at 105 K of Spin-Orbit Coupled Iridium Oxide $Ca_5Ir_3O_{12}$

Hiroki Hanate[1][*], Takumi Hasegawa[2], Satoru Hayami[3], Satoshi Tsutsui[45], Shoya Kawano[1], and Kazuyuki Matsuhira[1][†]

[1] *Graduate School of Engineering, Kyushu Institute of Technology, Kitakyushu 804-8550, Japan*

[2] *Graduate School of Integrated Arts and Sciences, Hiroshima University, 1-7-1 Kagamiyama, Higashi-Hiroshima 739-8521, Japan*

[3] *Department of Applied Physics, The University of Tokyo, Tokyo 113-8656, Japan*

[4] *Japan Synchrotron Radiation Research Institute (JASRI), SPring-8, Sayo, Hyogo 679-5198, Japan*

[5] *Institute of Quantum Beam Science, Graduate School of Science and Engineering, Ibaraki University, Hitachi, Ibaraki 316-8511, Japan*

We report the inelastic X-ray scattering (IXS) experimental results of iridium oxide $Ca_5Ir_3O_{12}$ with a strong spin-orbit interaction, showing the hidden order at 105 K where no superlattice reflections were observed so far. We measured the IXS spectra of $Ca_5Ir_3O_{12}$ along Γ-A, Γ-M, Γ-K-M, M-L, and K-H directions in the Brillouin zone of a hexagonal lattice down to 20 K. The obtained phonon spectra show almost no change on cooling; there are no soft phonon modes. However, the superlattice reflections specified by wavevector $\mathbf{q}=(1/3, 1/3, 1/3)$ are observed below 105 K. For the order parameter in the hidden order, the characteristic on intensity for observed superlattice reflections can lead to the irreducible representation A_2 order parameter in the point group $31m$. Furthermore, the theoretical study indicates that the hidden order at 105 K comes from an electric toroidal dipole or higher-order multipole ordering.

One of main topics in solid state physics is to reveal the order parameter (OP) of phase transition. In particular, revealing new type of order parameters leads to a

discover of new physics and a development of new functions. Some spin-orbit-coupled materials show a phase transition in which the OP cannot be specified, despite efforts to elucidate the OP of the phase transition. They are called "hidden order". In a typical "hidden order", despite the observable fact that the specific heat shows a large anomaly and a large entropy change exists, it is difficult to specify the OP even by various experimental methods. Such a hidden phase transition is expected to be seen when the order parameters are the higher order moments (so-called multipole) than the dipole, and its conjugate external field response is not available and cannot be directly detected.[1,2] A typical example is the phase transition at 17.5 K in URu_2Si_2, which has been elucidated since the discovery of the phase transition in 1987, but no conclusion has been reached yet.[1,2] Recently, for hidden order candidates, phase transitions due to electric toroidal (ET) multipole have been theoretically proposed for some materials such as $Cd_2Re_2O_7$, $CeCoSi$, $PrIr_2Zn_{20}$, $PrRh_2Zn_{20}$ and PrV_2Al_{20}.[3–7] These phase transitions are phase transitions that break the spatial inversion symmetry in the low temperature phase, and it is possible to specify the OP by the response caused by the phase transition, the new cross-correlation response, and the non-reciprocal response.

In this paper, we report the discovery of a new ET ordering candidate $Ca_5Ir_3O_{12}$. $Ca_5Ir_3O_{12}$ has been actively studied as a quasi-one-dimensional spin-orbit coupled material. The crystal structure is a non-centrosymmetric hexagonal structure with a space group of $P\bar{6}2m$,[8,9] and the primitive lattice includes three one-dimensional (1D) chains of the edge-sharing IrO_6; the three 1D rods form triangular lattices. Three Ir sites are equivalent in this primitive lattice; the averaged valence of Ir ions is +4.67. $Ca_5Ir_3O_{12}$ exhibits semi-conductivity and has two phase transitions while changing the temperature.[8] Lower one is an antiferromagnetic ordering below 7.8 K,[8,10,11] and the other is a second-order phase transition at $T_s = 105$ K, where the specific heat clearly indicates an anomaly, and the electrical resistivity shows a sharp upward bend at T_s.[8,10,12] Presently, the origin of the phase transition at T_s is not clear, because the structural and magnetic transitions for the powder samples have not been confirmed via XRD, neutron scattering, and μSR experiments;[8,11] the phase transition at T_s is "hidden order".

Our motivation is to clarify the origin of phase transition at T_s. These powder diffraction experiments may not have been able to detect the structural change due to this hidden order because the change of structure is very small. Furthermore, as the crystal structure of $Ca_5Ir_3O_{12}$ does not have spatial inversion symmetry, the above-mentioned responses caused by a phase transition that breaks the spatial inversion

symmetry might not be used to detect the phase transition of $Ca_5Ir_3O_{12}$; this is a more hidden order. The origin of the second-order phase transition at T_s is unlikely to be a simple structural phase transition, and there is a possibility of a phase transition due to the degree of freedom of the electron system. Recently, we performed Raman scattering measurement to understand the phase transition at T_s.[13] Since the Raman spectra clearly change below T_s, the symmetry of crystal structure changes in the phase transition at T_s. The observed energy range and polarization dependence of the spectral change indicate that oxygens in c-plane are involved in the phase transition at T_s. However, in Raman spectroscopy, only Raman active mode at $\mathbf{q} = 0$ is observable, it is difficult to specify the structural phase transition. Therefore, the IXS measurement would be effective in the search for specific superlattice instability, because it can be accessible to the details of $\mathbf{q} \neq 0$ modes.

The IXS measurements were carried out at BL35XU of SPring-8 using ~ 1.5 meV resolution at 21.7 keV corresponding to Si (11 11 11) reflection.[14] The sample used in this experiment was the same as one used in Ref. 15, which was grown by the $CaCl_2$ flux methods. The momentum resolution is (0.04 0.10 0.046) [r.l.u.]. The sample was cooled using a He closed-cycle cryostat mounted within the Huber 512.1 Eulerian cradle.[16] To compensate for the offset of the energy transfer, the Stokes and anti-Stokes components were measured.

Before reporting the new results, we will summarize the results of IXS at room temperature (RT). IXS spectra of $Ca_5Ir_3O_{12}$ were measured along Γ-A, Γ-M, and Γ-K-M directions in the Brillouin zone of a hexagonal lattice at RT.[15] The phonon dispersions obtained below 40 meV are in a good agreement with the results of calculation by generalized gradient approximation with spin-orbit interaction (SO-GGA) for $1 \times 1 \times 3$ supercell. The optical modes related to the Ir and Ca ions are observed near 10-20 and 20-40 meV, respectively. In the experimental results, there is no sign of softening at the A, K, and M points at RT.

The IXS spectra of $Ca_5Ir_3O_{12}$ along the some high symmetry $\mathbf{q}$-paths (Γ-K-M, Γ-M, K-H, and M-L) are shown in Figs. 1(b)-(e), and the exact measured $\mathbf{q}$ values are shown in Fig. 1(a). In each of Figs. 1(b)-(e), the temperature dependence of the spectra at four different $\mathbf{q}$ values is depicted. The data of the spectra along the Γ-K-M and Γ-M at RT are from Ref. 15. As shown in Figs. 1(b)-(e), the observed spectra do not show any temperature dependence except for the contribution of the Bose factor to the phonon peak intensities. The phonon peak positions at any $\mathbf{q}$ values hardly
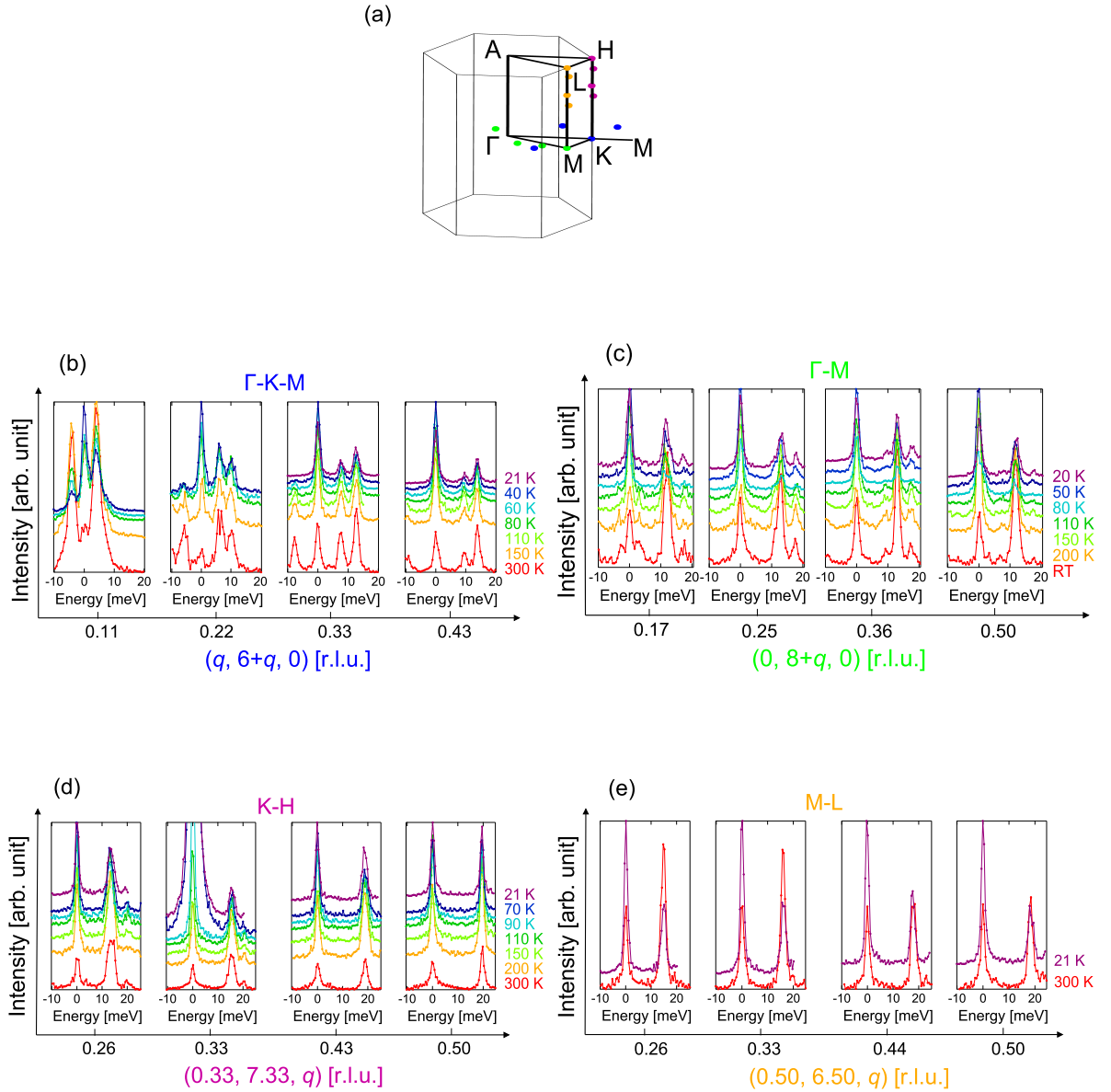
Fig. 1. (Color online) (a) Brillouin zone of $Ca_5Ir_3O_{12}$ (thin lines) and high symmetry **q**-path (thick line). Circles represent exact measured **q** in (b)-(e). (b)-(e) **q**-dependence of IXS spectra, obtained for $\mathbf{Q} \sim (q, 6+q, 0)$ (b), $(0, 8+q, 0)$ (c), $(0.33, 7.33, q)$ (d), and $(0.50, 6.50, q)$ (e). IXS spectra are color-coded by temperature.

depend on the temperature within the experimental error, indicating that there is no soft phonon mode. In contrast, the elastic peak intensity at $\mathbf{q} = (0.33, 0.33, 0.33)$ (Fig. 1(d)) changes more rapidly with temperature than that at other **q** values, as shown in Fig. 2. In particular, the peak intensity at $\mathbf{q} = (0.33, 0.33, 0.33)$ increases below 100 K, which is very close to $T_s = 105$ K. Below T_s, a superlattice structure is
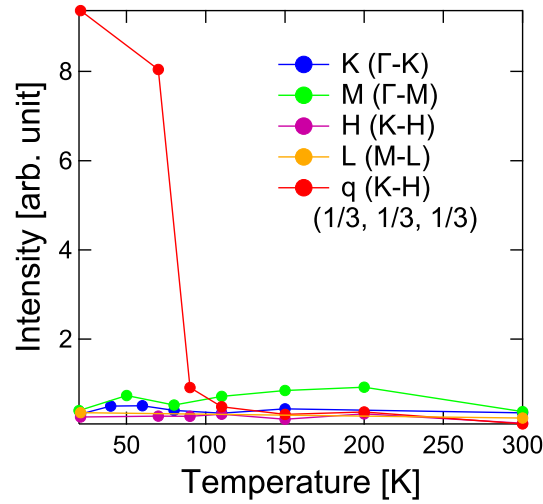
Fig. 2. (Color online) Temperature dependence of the elastic peak intensities in Figs. 1(b)-(e) of the some high symmetry **q**-points (K, M, H, and L) and **q** = (0.33, 0.33, 0.33).

expected, where the elastic peak intensity increases with decreasing temperature. The temperature dependence of the ϕ-scan profile at $\mathbf{Q}$ =(0.33, 7.33, 0.33) is shown in Fig. 3(a), where ϕ-scan is the scan whose rotational axis is parallel to the axis from the measuring sample to the cold head of the cryostat mounted on the Eulerian Cradle of the IXS spectrometer at BL35XU. A continuous increase of the superlattice peak below 100 K is confirmed. Therefore, this result indicates the existence of a $\sqrt{3}a \times \sqrt{3}a \times 3c$ superlattice. Fig. 3(b) shows the temperature dependence of the integrated intensity of the superlattice reflection at $\mathbf{Q}$ = (0.33, 7.33, 0.33) as shown in Fig. 3(a).

To investigate the details of this superlattice reflection, the ϕ-scan was employed. Thanks to the analyzer optics installed at BL35XU for the IXS measurements, the superlattice reflections were observed without background intensities. Figure 4(a) shows the ϕ-scan profile at 20 K at $\mathbf{Q}_{0n0} \sim (0, n, 0) + (0.33, 0.33, 0.33)$ (n = 6, 7, 8, 9, 10, and 11) and $\mathbf{Q}_{nn0} \sim (n, n, 0) + (0.33, 0.33, 0.33)$ (n = 3, 4, 5, and 6) . There is clearly a superlattice reflection at $\mathbf{Q}_{0n0}$, while the reflections at $\mathbf{Q}_{nn0}$ is much weaker.

The absence of the super-lattice reflections at $\mathbf{Q}_{nn0}$ leads to a restriction to the space group below T_s. Its crystal momentum is $\mathbf{q} = (1/3, 1/3, 1/3)$. The symmetry group of $\mathbf{q}$ is the point group $31m$. The OP can be classified by the irreducible representations of the point group $31m$, i.e. A_1, A_2, and E. If we describe the amplitude of the OP by u, then the intensity of the super-lattice reflections are usually proportional to u^2. However, if the OP belongs to A_2, we can derive that the intensity at $\mathbf{Q}_{nn0}$ is not
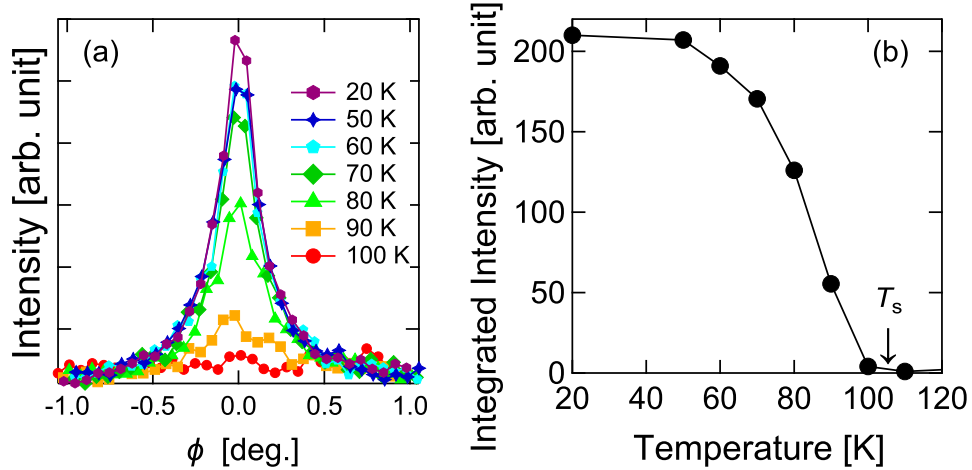
Fig. 3. (Color online) (a) Temperature dependence of ϕ-scan profile at $\mathbf{Q} = (0.33, 7.33, 0.33)$. (b) Temperature dependence of the integrated intensity of the superlattice reflection at $\mathbf{Q} = (0.33, 7.33, 0.33)$.

proportional to u^2, but to u^4 (see Supplement A[17]). This means that the intensity at $\mathbf{Q}_{nn0}$ is much weak with respect to the intensity at $\mathbf{Q}_{0n0}$, whose intensity is proportional to u^2. Therefore, the above-mentioned discussion of intensity by A_2 OP can explain successfully the present observation shown in Fig. 4. If we think about A_1 and E OPs, then there is no such different intensity. Therefore, the present result suggests that the OP belongs to the irreducible representation A_2.

We discuss the crystal structure below T_s caused by the A_2 OP. The phonon modes at $\mathbf{q} = (1/3, 1/3, 1/3)$ are classified as $12A_1 + 8A_2 + 20E$ by the point group $31m$. Since all atoms are involved in those eight A_2 modes, it is difficult to restrict what structure is derived from the A_2 OP. The recent study of Raman scattering experiment[13] has discussed the structure below T_s. It suggests the displacement of the O(1) atoms in the c plane. According to this suggestion, we will describe the structural change by the displacement of the O(1) atoms. The displacements of the other atoms are described in Supplement B.[18] According to the Landau theory, we can obtain three structures with $R3$, $P\bar{6}$, or $P312$ space groups from the A_2 OP (see Supplement C in detail[19]). The structure discussed below is an example, and the actual structure will be determined by future diffraction experiments. All discussions are based on the symmetry of the irreducible representation A_2 and do not depend on the structural details.

We discuss two perspectives on the structure below T_s. One is that the Raman
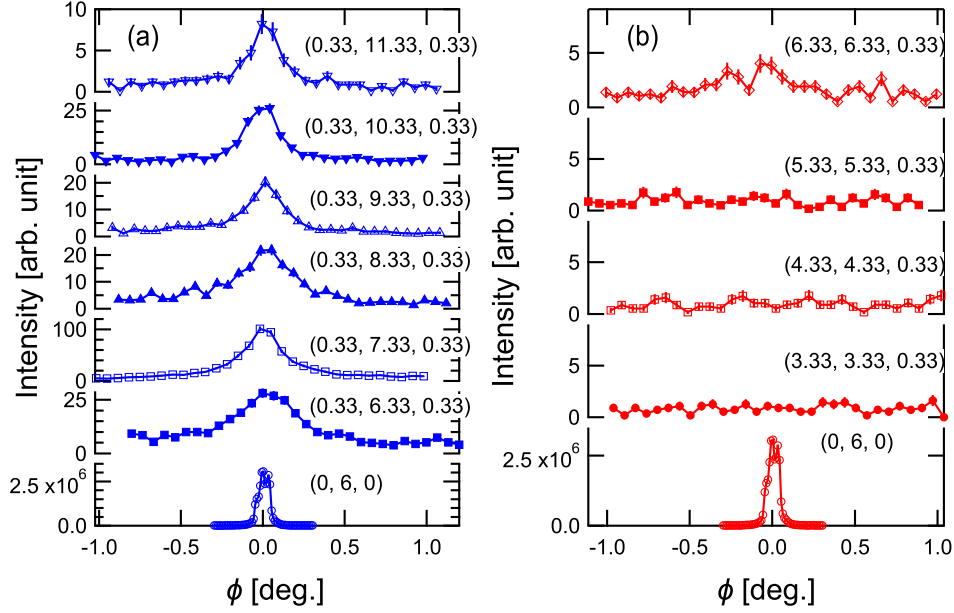
Fig. 4. (Color online) The ϕ-scan profile at 20 K (a) at $\mathbf{Q}_{0n0} \sim (0, n, 0) + (0.33, 0.33, 0.33)$ (n=6, 7, 8, 9, 10, and 11) and (b) at $\mathbf{Q}_{nn0} \sim (n, n, 0) + (0.33, 0.33, 0.33)$ (n=3, 4, 5, and 6). The origin of ϕ is defined by the center of reflection peak.

scattering experiment did not show a $\bar{6}$ symmetry breaking.[13] This suggests a $P\bar{6}$ structure. However, Raman scattering could not detect a super-lattice structure along the c-axis direction. Similarly, this would not be conclusive evidence of $P\bar{6}$, as it may not have detected m_z symmetry breaking. Another point of view is that the IrO$_6$ chain will remain one type after the phase transition. If there are multiple types of IrO$_6$ chains, the IrO$_6$ chains themselves will move, which will result in the large displacement of Ir and the superlattice reflection will be easily observed. However, the superlattice reflection intensity is small, so it is natural that the IrO$_6$ chain remains one type. In Raman scattering result,[13] the vibrational mode of the IrO$_6$ chain is observed as $A'_1(1)$, but no anomaly is observed in both width and energy, and no new peak is observed near this energy. From the result, it is expected that the IrO$_6$ chain remains one type. There are three types of IrO$_6$ chains in $P\bar{6}$ and $P312$, while one type in $R3$. Therefore, considering the type of IrO$_6$ chain, the $R3$ structure is plausible.

We introduce an example of the $R3$ structure, which is shown in Fig. 5. The other possible structures are discussed in Supplement C.[19] The size of its unit cell is $\sqrt{3}a \times \sqrt{3}a \times 3c$ in the hexagonal coordinate, and three primitive cells are included in the hexagonal unit cell. In the hexagonal unit cell, there are nine IrO$_6$-chains. If we think a bundle of three chains, which exchange each other by a 3-fold axis, there are three

bundles. The displacement of O(1) atoms is described by a rotation around the 3-fold axis in one bundle. In Fig. 5, the displacements of the rotation are 0, −1, and +1 in the three bundles. The structure is also tripled along the c-axis. Proceeding in the c-axis, the displacement of the rotation appears in the order of 0, −1, and +1. These displacements satisfies the translational symmetries of the rhombohedral lattice. The three bundles are identical according to the translational symmetries, and three chains in each bundle are identical according to the 3-fold axis. Therefore, there is one type of IrO_6 chain in this $R3$ structure.

Now, we consider a possibility of a valence order transition. The average valence of Ir is +4.67. Then, there is the possibility that a valence order of +5, +5, and +4 will happen. In such valence order, the OP is a valence fluctuation of Ir ions. The irreducible representations of such fluctuation are $A_1 + E$ in the point group $31m$ at $\mathbf{q} = (1/3, 1/3, 1/3)$. Since they do not include A_2, the observed order parameter will not be valence fluctuation such as charge order and conventional CDW; no CDW soft mode is also observed. Under the order by A_2, a valence order belonging to A_1 is possible. However, this is not the OP, but induced by the A_2 OP.

The observed super-lattice reflections will be explained by the structural change belonging to the irreducible representation A_2. This means the transition is a structural transition. Therefore, we expect a soft mode to derive the structural transition. However, in the present experiments, we did not find any soft mode at $\mathbf{q} = (1/3, 1/3, 1/3)$. The lack of a soft mode suggests that the transition is an order-disorder type structural transition. In this case, some local distortions exist above T_s. The transition occurs at T_s by a long-range order of such local distortions. An evidence of a local distortion is that the resistivity is semi-conductive above T_s. This means that charges are trapped locally by some local distortion above T_s. Another evidence has been reported by Raman experiment.[13] That is observed by a broad additional peak above T_s. These local distortions will be fluctuate in time and in space. They will be observed as a diffuse scattering by a diffraction experiment. The diffuse scattering is observed as a broad signal around $\mathbf{Q}_{0n0}$ above T_s, and becomes sharp near T_s. Then, it is a Bragg peak below T_s. In this case, a soft mode does not necessarily have to be observed. This diffuse scattering will be verified by a X-ray diffraction experiment using a single crystal, which is a future subject.

The above data imply that the OP at T_s corresponds to the A_2 mode, where space group changes from $P\bar{6}2m$ (#189) to $P\bar{6}$ (#174) when supposing the $\bar{6}$ symmetry or
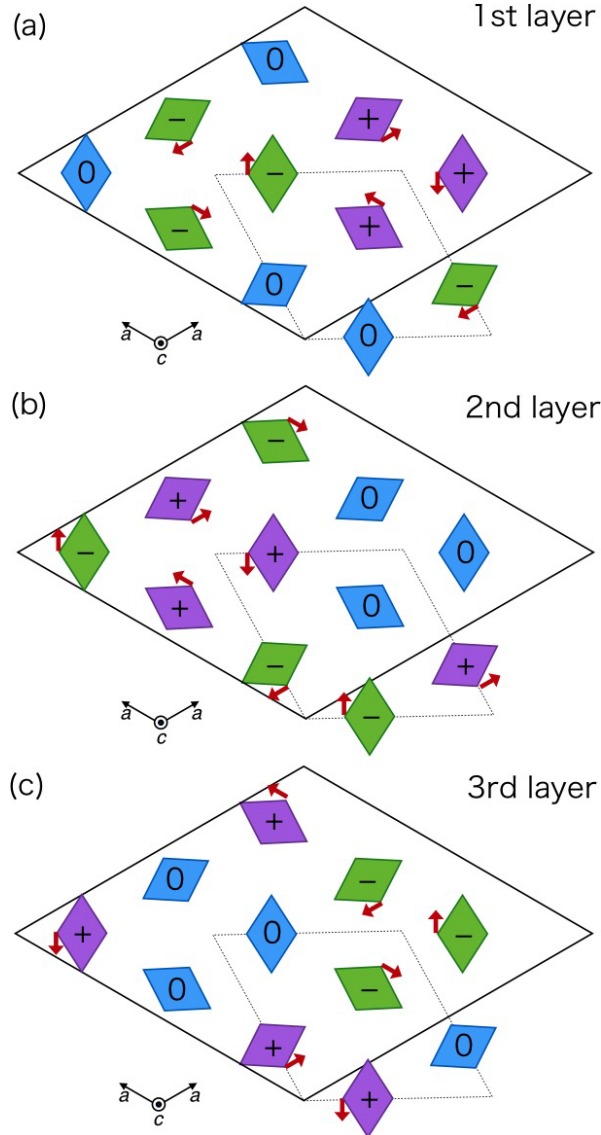
Fig. 5. (Color online) An example superlattice structure by the A_2 OP. We show only IrO_6 octahedron with displacements of O(1) atoms; the displacement is indicated by a length-enhanced arrow. The size of its unit cell is $\sqrt{3}a \times \sqrt{3}a \times 3c$; the broken line shows the size of unit cell in $P\bar{6}2m$ (#189). (a) The 1st layer from $z = 0.0$ to 0.33; this is labelled by A. This is the same as the 3rd layer from $z = 0.67$ to 1.0. (b) The 2nd layer from $z = 0.33$ to 0.67; this is labelled by B. (c) The 3rd layer from $z = 0.67$ to 1.0; this labelled by C. This superlattice structure is formed by stacking ABC along c-axis. The sign shown on IrO_6 octahedron corresponds to the sign of the z component of the ET dipole. The "0" shown on IrO_6 means that the displacements of the two O(1) atoms are in opposite directions, and z component of the ET dipole is cancelled.

to $R3$ (#146) without $\bar{6}$. The origin of this phase transition might be attributed to the activation of the ET dipole or higher-order multipoles belonging to the same irreducible representation.[20] In fact, the displacements of the O(1) atoms give a nonzero ET dipole

moment $\mathbf{r}_i \times \boldsymbol{\delta}_i$ around the Ir ions along the z direction, where $\mathbf{r}_i$ is the position vector and $\boldsymbol{\delta}_i$ is the displacement vector from the positions at the ith Ir ion in the higher-temperature phase, when setting each Ir ion as the origin.[13] In other words, each Ir ion is affected by an axial vector field along the z axis that arises from the ET dipole.[21, 22] From the development of the reflection at $(1/3, 1/3, 1/3)$, the alignments of the ET dipole along the z axis are the up-down-zero structure and three-sublattice trimers in the c plane are also aligned in the up-down-zero structures in the case of $R3$, as shown in Fig. 5. Thus, the phase transition at T_s is regarded as the density waves of the ET dipole degree of freedom.

Microscopically, such an axial field at each Ir ion can induce an effective spin-orbit entanglement in the expression of $\mathbf{l}_i \times \mathbf{s}_i$, where $\mathbf{l}_i$ and $\mathbf{s}_i$ are the atomic orbital-angular and spin-angular momenta, respectively, which has the same symmetry as the above axial ET dipole.[23, 24] Such a peculiar spin-orbit coupling can become active as local atomic or bond degrees of freedom. The investigation to clarify which electronic degrees of freedom play an important role will be left for future theoretical study.

The ET dipole gives rise to intriguing responses to external stimuli. For example, the thermoelectric power tensor (Seebeck effect), where the electric field E_μ is induced by a thermal gradient $\boldsymbol{\nabla}_\nu T$ as $E_\mu = \beta_{\mu\nu}\boldsymbol{\nabla}_\nu T$ ($\mu, \nu = x, y, z$) would be a good probe for the ET dipole. As $\beta_{\mu\nu}$ is the rank-2 polar tensor of time-reversal even, the rank-1 ET dipole contributes to the tensor in the form of $\beta_{xy} = -\beta_{yx}$. Furthermore, the ET dipole would also be detected though the measurements for other physical phenomena, such as the Nernst effect, spin-current generation, and the magnetic resistance, which includes the contribution from the ET dipole.

In this letter, we report the IXS spectra of $Ca_5Ir_3O_{12}$ down to 20 K from RT, in order to reveal the OP of hidden order at $T_s = 105$ K. The superlattice reflections specified by wavevector $\mathbf{q}=(1/3, 1/3, 1/3)$ are observed below T_s although the obtained phonon spectra are not changed on cooling; this is a first observation superlattice reflections in this hidden order. From the consideration of intensity for the candidate structural symmetry at low temperature phase, the OP in the hidden order belongs to the irreducible representation A_2. The theoretical study indicates that this hidden order at 105 K comes from an ET dipole or higher-order multipole ordering.

References

1) T. T. M. Palstra, , A. A. Menovsky, J. van den Berg, A. J. Dirkmaat, P. H. Kes, G. J. Nieuwenhuys and J.A. Mydosh, Phys. Rev. Lett. **55**, 2727 (1985).

2) J. A. Mydosh and P. M. Oppeneer, Philosophical Magazine **94**, 3642 (2014).

3) L. Fu, Phys. Rev. Lett. **115**, 026401 (2015).

4) S. Di Matteo and M. R. Norman, Phys. Rev. B **96**, 115156 (2017).

5) S. Hayami, Y. Yanagi, H. Kusunose, and Y. Motome, Phys. Rev. Lett. **122**, 147602 (2019).

6) M. Yatsushiro and S. Hayami, J. Phys. Soc. Jpn. **89**, 013703 (2020).

7) T. Ishitobi and K. Hattori, J. Phys. Soc. Jpn. **88**, 063708 (2019).

8) M. Wakeshima, N. Taira, Y. Hinatsu, Y. Ishii, Solid State Commun., **125**, 311 (2003).

9) R.F. Sarkozy, W. Moeller, B.L. Chamberland, J. Solid State Chem. **9**, 242 (1974).

10) G. Cao, V. Durairaj, S. Chikara, S. Parkin, and P. Schlottmann, Phys Rev. B, **75**, 134402 (2007).

11) I. Franke, P.J. Baker, S.J. Blundell, T. Lancaster, W. Hayes, F.L. Pratt, G. Cao, Phys Rev. B, **83**, 094416 (2011).

12) K. Matsuhira, K. Nakamura, Y. Yasukuni, Y. Yoshimoto, D. Hirai, and Z. Hiroi, J. Phys. Soc. Jpn. **87**, 013703 (2018).

13) T. Hasegawa, W. Yoshida, K. Nakamura, N. Ogita, K. Matsuhira, J. Phys. Soc. Jpn. **89**, 054602 (2020).

14) A. Q. R. Baron, Y. Tanaka, S. Goto, K. Takeshita, T. Matsushita, and T. Ishikawa, J. Phys. Chem. Solids **61**, 461 (2000).

15) H. Hanate, T. Hasegawa, S. Tsutsui, K. Nakamura, Y. Yoshimoto, N. Kishigami, S. Haneta, and K. Matsuhira, J. Phys. Soc. Jpn. **89**, 053601 (2020).

16) https://www.xhuber.com/en/product-groups/1-components/12-rotation/eulerian-cradles/

17) (Supplemental material A) Scattering factor of X-ray diffraction for A_2 modes is calculated and discussed.

18) (Supplemental material B) Atomic displacement consisting of the first-order terms of the order-parameter is described.

19) (Supplemental material C) Landau theory with A_2 mode is considered.

20) S. Hayami, M. Yatsushiro, Y. Yanagi, and H. Kusunose, Phys. Rev. B **98**, 165110 (2018).

21) V. M. Dubovik and V. V. Tugushev, Phys. Rep. **187**, 145 (1990).

22) Although the in-plane component of the electric toroidal dipole is also induced for each Ir ion, it is canceled out in the unit cell.

23) S. Hayami and H. Kusunose, J. Phys. Soc. Jpn. **87**, 033709 (2018).

24) H. Kusunose, R. Oiwa, and S. Hayami, J. Phys. Soc. Jpn. **89**, 104704 (2020).

Supplement A. Scattering factor of X-ray diffraction for the A_2 modes.

We consider the following scattering factor of X-ray diffraction.

$$
\begin{aligned}
F(\mathbf{Q}) &= \sum_{i,a} f_i(\mathbf{Q}) e^{2\pi i \mathbf{Q}\cdot(\mathbf{r}_{ia}+\mathbf{u}_{ia})} \tag{1}\\
&= \sum_{i,a} f_i(\mathbf{Q}) e^{2\pi i \mathbf{Q}\cdot\mathbf{r}_{ia}} \left(1 + 2\pi i(\mathbf{Q}\cdot\mathbf{u}_{ia}) - 2\pi^2(\mathbf{Q}\cdot\mathbf{u}_{ia})^2 + \dots\right) \tag{2}\\
&= F^{(0)}(\mathbf{Q}) + F^{(1)}(\mathbf{Q}) + F^{(2)}(\mathbf{Q}) + \dots. \tag{3}
\end{aligned}
$$

where, a is an index of a unit cell, i is an index of an atom in the a-th unit cell, $f_i(\mathbf{Q})$ is the atomic form factor of the i-th atom, $\mathbf{r}_{ia}$ is the position of the (ia)-th atom in the $P\bar{6}2m$ structure above T_{s}, and $\mathbf{u}_{ia}$ is the displacement of the (ia)-th atom below T_{s}. $F^{(n)}(\mathbf{Q})$ is the summation of the n-th power terms of $\mathbf{u}_{ia}$. $F^{(0)}(\mathbf{Q}) \neq 0$, if $\mathbf{Q}$ is a reciprocal lattice vector $\mathbf{G}$. Since $\mathbf{u}_{ia}$ has a factor $\exp(2\pi i \mathbf{q}\cdot\mathbf{r}_{ia})$, $F^{(1)}(\mathbf{Q}) \neq 0$, when $\mathbf{Q} + \mathbf{q} = \mathbf{G}$. Similarly, $F^{(2)}(\mathbf{Q}) \neq 0$, if $\mathbf{Q} + \mathbf{q}_1 + \mathbf{q}_2 = \mathbf{G}$, where $\mathbf{q}_1$ and $\mathbf{q}_2$ are wavevectors of the $\mathbf{u}_{ia}$.

The X-ray diffraction intensity is proportional to $|F(\mathbf{Q})|^2$. If we think $\mathbf{Q}_{nn0} = (n + 1/3, n + 1/3, 1/3)$, then, $F^{(0)}(\mathbf{Q}_{nn0}) = 0$, $F^{(1)}(\mathbf{Q}_{nn0}) \neq 0$ with $\mathbf{q} = (2/3, 2/3, 2/3)$ and $F^{(2)}(\mathbf{Q}_{nn0}) \neq 0$ with $\mathbf{q}_1 = \mathbf{q}_2 = (1/3, 1/3, 1/3)$. Usually, the leading term of the intensity will be $|F^{(1)}(\mathbf{Q}_{nn0})|^2$ with u^2. Now, we show $|F^{(1)}(\mathbf{Q}_{nn0})|^2 = 0$, if $\mathbf{u}_{ia}$ belongs to the A_2 irreducible representation.

In the space group $P\bar{6}2m$, there is the mirror m_n operation which does not change $\mathbf{Q}_{nn0}$. The mirror plane is perpendicular to $\mathbf{a}^* - \mathbf{b}^*$ direction, where $\mathbf{a}^*$ and $\mathbf{b}^*$ are the reciprocal lattice vectors. By this m_n operation, $F(\mathbf{Q}_{nn0})$ does not change, since both of $(\mathbf{u}_{ia}\cdot\mathbf{Q}_{nn0})$ and $(\mathbf{Q}_{nn0}\cdot\mathbf{r}_{i,a})$ do not change.

We suppose that the (ia)-th atom moves to (jb)-th position under the m_n operation. In other words, $m_n\mathbf{r}_{ia} = \mathbf{r}_{jb}$. And also $m_n\mathbf{r}_{jb} = \mathbf{r}_{ia}$. Then, we consider the following summation.

$$
\begin{aligned}
F_1^{(1)} &= f_i(\mathbf{Q}_{nn0})(\mathbf{u}_{ia}\cdot\mathbf{Q}_{nn0}) e^{2\pi i \mathbf{Q}_{nn0}\cdot\mathbf{r}_{ia}}\\
&\quad + f_j(\mathbf{Q}_{nn0})(\mathbf{u}_{jb}\cdot\mathbf{Q}_{nn0}) e^{2\pi i \mathbf{Q}_{nn0}\cdot\mathbf{r}_{jb}} \tag{4}\\
&= f(\mathbf{Q}_{nn0}) \left\{(\mathbf{u}_{ia}\cdot\mathbf{Q}_{nn0}) + (\mathbf{u}_{jb}\cdot\mathbf{Q}_{nn0})\right\} e^{2\pi i \theta}, \tag{5}
\end{aligned}
$$

where, $\theta = \mathbf{Q}_{nn0}\cdot\mathbf{r}_{ia} = \mathbf{Q}_{nn0}\cdot\mathbf{r}_{jb}$, $f(\mathbf{Q}_{nn0}) = f_i(\mathbf{Q}_{nn0}) = f_j(\mathbf{Q}_{nn0})$ since i and j are the same chemical element. Now, we think the irreducible representation A_2 of the point group $31m$. The point group $31m$ is the symmetry group of $\mathbf{q} = (1/3, 1/3, 1/3)$. From the character table of the A_2, the character of m_n is -1. This means the following relation.

$$
m_n\mathbf{u}_{ia} = -\mathbf{u}_{jb}. \tag{6}
$$

When we take inner-product of both sides with $\mathbf{Q}_{nn0}$, we derive,

$$
m_n(\mathbf{u}_{ia}\cdot\mathbf{Q}_{nn0}) = (\mathbf{u}_{ia}\cdot\mathbf{Q}_{nn0}) = -(\mathbf{u}_{jb}\cdot\mathbf{Q}_{nn0}). \tag{7}
$$

If we substitute them in $F_1^{(1)}$, we can get $F_1^{(1)} = 0$. On the other hand, if the (ia)-th atom locates on the mirror plane, then, $m_n \mathbf{u}_{ia} = -\mathbf{u}_{ia}$. In this case, the atomic displacement, $\mathbf{u}_{ia}$, is perpendicular to the mirror. We get $(\mathbf{u}_{ia} \cdot \mathbf{Q}_{nn0}) = 0$. From these results, $F^{(1)}(\mathbf{Q}_{nn0}) = 0$, if $\mathbf{u}_{ia}$ belongs to A_2. $F^{(1)}(\mathbf{Q}_{nn0})$ is the leading order term of the X-ray scattering factor with respect to the $\mathbf{u}_{ia}$. The next term $F^{(2)}(\mathbf{Q}_{nn0})$ is a summation of $(\mathbf{u}_{ia} \cdot \mathbf{Q}_{nn0})^2$, and does not vanish. Therefore, the intensity $|F(\mathbf{Q}_{nn0})|^2$ is proportional to u^4. Since this is higher order than other $\mathbf{Q}$, the intensity is very weak, when $|u|$ is small.

The index $1/3$ is important for the conclusion of the u^4 intensity. If we think a $1/2$ case, then, the wavevector of the second-order terms do not include $1/2$. Therefore, the u^4 contribution to the intensity is absent, if a mirror operation doesn't change $\mathbf{Q}$ and converts $\mathbf{u}_{ia}$ to $-\mathbf{u}_{ia}$. In such case, the space group of the distorted structure consists of a glide plane, which guarantees the intensity is 0. In the present case with $1/3$, the intensity of $\mathbf{Q}_{nn0}$ is small, but not 0. This is useful to discuss the symmetry of the order-parameter, when the distortion is small. When the distortion becomes large, the intensity at $\mathbf{Q}_{nn0}$ could be the same order as that at $\mathbf{Q}_{0n0}$.

If we think about $\mathbf{Q}_{0n0} = (1/3, n+1/3, 1/3)$, there is no symmetric operation conserving $\mathbf{Q}_{0n0}$. Then, there is no reason that the intensity at $\mathbf{Q}_{0n0}$ is weak. If we think about A_1 and E, they have no symmetric operation which multiplies $\mathbf{u}_{ia}$ by -1. Then, we can not expect that the intensity at $\mathbf{Q}_{nn0}$ is weak for A_1 and E. Therefore, only if the order-parameter belongs to A_2, the intensity at $\mathbf{Q}_{nn0}$ becomes very weak in comparison to that at $\mathbf{Q}_{0n0}$.

Supplement B. Atomic displacement consisting of the first-order terms of the order-parameter

We consider atomic displacement of the distorted structure below T_s, assumed that the order-parameter is the A_2 mode at the wavevector $\mathbf{q}_1$. As discussed in Supplement B [1], the realized lattice is rhombohedral or hexagonal. In the case of the rhombohedral lattice, there are two new reciprocal lattice vectors, $\mathbf{q}_1$ and $\mathbf{q}_1'$. The volume is three times larger. In the case of the hexagonal lattice, in addition to the four vectors of $\mathbf{q}_1$, $\mathbf{q}_1'$, $\mathbf{q}_2$, and $\mathbf{q}_2'$, the another four vectors, $(0, 0, 1/3)$, $(0, 0, 2/3)$, $(1/3, 1/3, 0)$, and $(2/3, 2/3, 0)$, become new reciprocal lattice vectors. The volume is nine times. Since $(0, 0, 1/3) = \mathbf{q}_2 - \mathbf{q}_1$, the contribution from $(0, 0, 1/3)$ is second-order of the order-parameter. Similarly, the wavevectors, $(0, 0, 2/3)$, $(1/3, 1/3, 0)$, $(2/3, 2/3, 0)$, and $(0, 0, 0)$, are second-order terms. Here, we think about the first-order terms with the wavevectors, $\mathbf{q}_1$, $\mathbf{q}_1'$, $\mathbf{q}_2$, and $\mathbf{q}_2'$.

In the point group $31m$, the freedom of the atomic displacements are decomposed into $12A_1 + 8A_2 + 20E$. Therefore, there are eight basis vectors of the atomic displacement belonging to A_2 at $\mathbf{q}_1$. This vectors are written as $\mathbf{w}_{1k,ia}$. The eight vectors are distinguished by k. The position of the origin of a-th unit cell is $\mathbf{R}_a$. Then, we can write the $\mathbf{R}_a$ dependence as,

$$\mathbf{w}_{1k,ia} = \mathbf{w}_{1k,i} e^{2\pi i \mathbf{q}_1 \cdot \mathbf{R}_a}. \tag{1}$$

The basis vectors at the other three wavevectors are defined as,

$$\mathbf{w}_{1'k,ia} = \mathbf{w}_{1k,i}^* e^{2\pi i \mathbf{q}_1' \cdot \mathbf{R}_a}, \tag{2}$$

$$\mathbf{w}_{2k,ia} = (m_z \mathbf{w}_{1k,i}) e^{2\pi i \mathbf{q}_2 \cdot \mathbf{R}_a}, \tag{3}$$

$$\mathbf{w}_{2'k,ia} = (m_z \mathbf{w}_{1k,i}^*) e^{2\pi i \mathbf{q}_2' \cdot \mathbf{R}_a}, \tag{4}$$

where, the mirror m_z perpendicular to the c axis operates only on $\mathbf{w}_{1k,i}$. Using these definitions, the atomic displacement $\mathbf{u}_{ia}$ is written as,

$$\mathbf{u}_{ia} = \sum_{x=1,1',2,2'} u_x \sum_k \xi_k \, \mathbf{w}_{xk,ia}. \tag{5}$$

The four coefficients u_x determine the structural distortion. We take them as the order-parameters. The free-energy as the function of u_x is described in Supplement C [1]. ξ_k determine the eigenvector of the order-parameter. If the structural change is caused by soft-modes, the soft modes are quadruple degenerate, and the eigenvectors of the soft-modes are $\sum_k \xi_k \, \mathbf{w}_{xk,ia}$.

The components of $\mathbf{u}_{ia}$ are real. This means $\mathbf{u}_{ia}^* = \mathbf{u}_{ia}$. To enforce this relation, we need to satisfy $u_1' = u_1^*$ and $u_2' = u_2^*$. When a symmetric operator g is applied to $\mathbf{w}_{xk,ia}$, we write the resulting vector at the ia-th atom as $(g\mathbf{w}_{xk})_{ia}$. From the character table of the point group $31m$, $\mathbf{w}_{xk,ia}$ belonging to A_2 is converted as,

$$(C_3 \mathbf{w}_{xk})_{ia} = \mathbf{w}_{xk,ia}, \quad (m_y \mathbf{w}_{xk})_{ia} = -\mathbf{w}_{xk,ia}. \tag{6}$$

1

In the cases of the residual symmetric operations in the space group $P\bar{6}2m$, m_z and C_{2x}, we can obtain the following relations from eqs. (2)-(4) and from $C_{2x} = m_z m_y$.

$$(m_z \mathbf{w}_{1k})_{ia} = \mathbf{w}_{2k,ia}, \quad (m_z \mathbf{w}_{1'k})_{ia} = \mathbf{w}_{2'k,ia}, \tag{7}$$

$$(m_z \mathbf{w}_{2k})_{ia} = \mathbf{w}_{1k,ia}, \quad (m_z \mathbf{w}_{2'k})_{ia} = \mathbf{w}_{1'k,ia}, \tag{8}$$

$$(C_{2x} \mathbf{w}_{1k})_{ia} = -\mathbf{w}_{2k,ia}, \quad (C_{2x} \mathbf{w}_{1'k})_{ia} = -\mathbf{w}_{2'k,ia}, \tag{9}$$

$$(C_{2x} \mathbf{w}_{2k})_{ia} = -\mathbf{w}_{1k,ia}, \quad (C_{2x} \mathbf{w}_{2'k})_{ia} = -\mathbf{w}_{1'k,ia}. \tag{10}$$

From these results, we can derive,

$$(C_3 \mathbf{u})_{ia} = \sum_k \xi_k \left(u_1 \mathbf{w}_{1k,ia} + u_{1'} \mathbf{w}_{1'k,ia} + u_2 \mathbf{w}_{2k,ia} + u_{2'} \mathbf{w}_{2'k,ia} \right), \tag{11}$$

$$(m_y \mathbf{u})_{ia} = \sum_k \xi_k \left(-u_1 \mathbf{w}_{1k,ia} - u_{1'} \mathbf{w}_{1'k,ia} - u_2 \mathbf{w}_{2k,ia} - u_{2'} \mathbf{w}_{2'k,ia} \right), \tag{12}$$

$$(m_z \mathbf{u})_{ia} = \sum_k \xi_k \left(u_2 \mathbf{w}_{1k,ia} + u_{2'} \mathbf{w}_{1'k,ia} + u_1 \mathbf{w}_{2k,ia} + u_{1'} \mathbf{w}_{2'k,ia} \right), \tag{13}$$

$$(C_{2x} \mathbf{u})_{ia} = \sum_k \xi_k \left(-u_2 \mathbf{w}_{1k,ia} - u_{2'} \mathbf{w}_{1'k,ia} - u_1 \mathbf{w}_{2k,ia} - u_{1'} \mathbf{w}_{2'k,ia} \right). \tag{14}$$

From these conversion relations, the eqs. (1)-(4) in the Supplement B for the order-parameters are obtained [1].

To describe the basis vectors $\mathbf{w}_{1k,ia}$, we define the positions of 20 atoms in the unit cell as shown in Table 1. We summarize the eight $\mathbf{w}_{1k,ia}$ in Table 2. Figure 1(a) and (b) in Supplement B corresponds to the imaginary part and real part of the structure of $\mathbf{w}_{1,4,ia}$ in the case that $\xi_4 = 1$ and $\xi_k = 0$, for $k \neq 4$ [1].

References

[1] (Supplemental material C) Landau theory with A_2 mode is considered.

[2] M. Wakeshima, N. Taira, Y. Hinatsu, Y. Ishii, Solid State Commun. **125**, 311(2003).

i	atom	position
1	Ca(1)	(1/3,2/3,0.5)
2	Ca(1)	(2/3,1/3,0.5)
3	Ca(2)	(-0.2873,0,0.5)
4	Ca(2)	(0,-0.2873,0.5)
5	Ca(2)	(0.2873,0.2873,0.5)
6	Ir	(0.3330,0,0)
7	Ir	(0,0.3330,0)
8	Ir	(-0.3330,-0.3330,0)
9	O(1)	(0.2006,0,0.5)
10	O(1)	(0,0.2006,0.5)
11	O(1)	(-0.2006,-0.2006,0.5)
12	O(2)	(0.4617,0,0.5)
13	O(2)	(0,0.4617,0.5)
14	O(2)	(-0.4617,-0.4617,0.5)
15	O(3)	(0.4460,0.2407,0)
16	O(3)	(-0.2407,0.2053,0)
17	O(3)	(-0.2053,-0.4460,0)
18	O(3)	(0.2053,-0.2407,0)
19	O(3)	(0.2407,0.4460,0)
20	O(3)	(-4460,-0.2053,0)

Table 1: The atomic positions of 20 atoms for the definition of $\mathbf{w}_{xk,ia}$. The values are taken from the neutron diffraction data.[2]

k	$\mathbf{w}_{1,k,i}$
1	$\mathbf{w}_{1,1,1} = (0,0,1)$, $\mathbf{w}_{1,1,2} = (0,0,-1)$
2	$\mathbf{w}_{1,2,3} = (1,2,0)$, $\mathbf{w}_{1,2,4} = (-2,-1,0)$, $\mathbf{w}_{1,2,5} = (1,-1,0)$
3	$\mathbf{w}_{1,3,6} = (1,2,0)$, $\mathbf{w}_{1,3,7} = (-2,-1,0)$, $\mathbf{w}_{1,3,8} = (1,-1,0)$
4	$\mathbf{w}_{1,4,9} = (1,2,0)$, $\mathbf{w}_{1,4,10} = (-2,-1,0)$, $\mathbf{w}_{1,4,11} = (1,-1,0)$
5	$\mathbf{w}_{1,5,12} = (1,2,0)$, $\mathbf{w}_{1,5,13} = (-2,-1,0)$, $\mathbf{w}_{1,5,14} = (1,-1,0)$
6	$\mathbf{w}_{1,6,15} = (1,2,0)$, $\mathbf{w}_{1,6,16} = (-2,-1,0)$, $\mathbf{w}_{1,6,17} = (1,-1,0)$ $\mathbf{w}_{1,6,18} = (1,2,0)$, $\mathbf{w}_{1,6,19} = (-2,-1,0)$, $\mathbf{w}_{1,6,20} = (1,-1,0)$
7	$\mathbf{w}_{1,7,15} = (1,0,0)$, $\mathbf{w}_{1,7,16} = (0,1,0)$, $\mathbf{w}_{1,7,17} = (-1,-1,0)$ $\mathbf{w}_{1,7,15} = (-1,0,0)$, $\mathbf{w}_{1,7,19} = (0,-1,0)$, $\mathbf{w}_{1,7,20} = (1,1,0)$
8	$\mathbf{w}_{1,8,15} = (0,0,1)$, $\mathbf{w}_{1,8,16} = (0,0,1)$, $\mathbf{w}_{1,8,17} = (0,0,1)$ $\mathbf{w}_{1,8,18} = (0,0,-1)$, $\mathbf{w}_{1,8,19} = (0,0,-1)$, $\mathbf{w}_{1,8,20} = (0,0,-1)$

Table 2: The eight basis vectors $\mathbf{w}_{xk,ia}$ belonging to A_2 irreducible representation. These basis vectors are not normalized. The components which are not shown are 0.

3

Supplement C. Landau theory with A_2 mode

We consider Landau theory, when the order-parameter belongs to A_2. The stars of $\mathbf{q}_1 = (1/3, 1/3, 1/3)$ are $\mathbf{q}_{1'} = (2/3, 2/3, 2/3)$, $\mathbf{q}_2 = (1/3, 1/3, 2/3)$, $\mathbf{q}_{2'} = (2/3, 2/3, 1/3)$. We define four complex numbers to each crystal momentum as u_1, $u_{1'}$, u_2, and $u_{2'}$. Since $\mathbf{q}_1 = -\mathbf{q}_{1'}$, $\mathbf{q}_2 = -\mathbf{q}_{2'}$, from the time-reversal symmetry, $u_{1'} = u_1^*$, $u_{2'} = u_2^*$. Then, it is sufficient to consider two complex numbers u_1 and u_2. These are converted by the symmetry operations in the space group $P\bar{6}2\mathrm{m}$ as followings.

$$
\begin{align}
C_3(u_1, u_2) &= (u_1, u_2), \tag{1}\\
m_y(u_1, u_2) &= (-u_1, -u_2), \tag{2}\\
m_z(u_1, u_2) &= (u_2, u_1), \tag{3}\\
C_{2x}(u_1, u_2) &= (-u_2, -u_1). \tag{4}
\end{align}
$$

For the discussion below, we describe as $u_1 = |u_1|e^{i\theta_1}$, $u_2 = |u_2|e^{i\theta_2}$. The relation between these parameters u_x and atomic displacements $\mathbf{u}_{ia}$ is described in Supplement C. Using these two complex numbers, we can expands the free energy as,

$$
\begin{align}
F &= \frac{A(T-T_s)}{2}(|u_1|^2 + |u_2|^2) + \frac{B}{4}(|u_1|^2 + |u_2|^2)^2 + \frac{C}{4}|u_1|^2|u_2|^2 \notag\\
&\quad + \frac{D}{6}(|u_1|^2 + |u_2|^2)^3 + \frac{E}{6}|u_1|^2|u_2|^2(|u_1|^2 + |u_2|^2) \notag\\
&\quad + \frac{G}{6}(u_1^6 + u_2^6) + \frac{G^*}{6}(u_{1'}^6 + u_{2'}^6) + \frac{H}{6}u_1^3 u_2^3 + \frac{H^*}{6}u_{1'}^3 u_{2'}^3 \notag\\
&\quad + \frac{I}{6}(u_1^3 u_{2'}^3 + u_{1'}^3 u_2^3) \tag{5}\\
&= \frac{A(T-T_s)}{2}(|u_1|^2 + |u_2|^2) + \frac{B}{4}(|u_1|^2 + |u_2|^2)^2 + \frac{C}{4}|u_1|^2|u_2|^2 \notag\\
&\quad + \frac{D}{6}(|u_1|^2 + |u_2|^2)^3 + \frac{E}{6}|u_1|^2|u_2|^2(|u_1|^2 + |u_2|^2) \notag\\
&\quad + \frac{|G|}{3}(|u_1|^6 \cos(6\theta_1 + \theta_G) + |u_2|^6 \cos(6\theta_2 + \theta_G)) \notag\\
&\quad + \frac{|H|}{3}|u_1|^3|u_2|^3 \cos(3(\theta_1 + \theta_2) + \theta_H) \notag\\
&\quad + \frac{I}{3}|u_1|^3|u_2|^3 \cos 3(\theta_1 - \theta_2). \tag{6}
\end{align}
$$

The coefficients G and H are complex number. $G = |G|e^{i\theta_G}$, and $H = |H|e^{i\theta_H}$. This is a result of the lack of the inversion symmetry. If the inversion symmetry exits, G and H must be real number. This system will undergo second-order transition at $T = T_s$, when $B > 0$. Here, we think that $|u_1|$ and $|u_2|$ is small so that the six-order terms are small with respect to the fourth-order terms. In this conditions, we get two superlattices: rhombohedral lattice, $(|u_1|, |u_2|) = (u, 0)$, or $(0, u)$, in the $C > 0$ case, and hexagonal lattice, $|u_1| = |u_2| = u/\sqrt{2}$, in the

1

space group	condition	u_1, u_2
$R3$	$C > 0$	$u_1 = 0$ or $u_2 = 0$
$P\bar{6}$	$C < 0$, and $I < 0$	$u_1 = u_2$
$P312$	$C < 0$, and $I > 0$	$u_1 = -u_2$

Table 1: The three structures obtained from the Free energy, eq. 6.

$C < 0$ case. Both lattices have the unit cell size of $\sqrt{3}a \times \sqrt{3}a \times 3c$, if we take the hexagonal unit cell. The volume is nine times larger than the $P\bar{6}2m$ structure. For the rhombohedral lattice, the hexagonal cell includes three primitive cells. The volume of the primitive cell is three times larger.

The sixth-order terms determine the phases, θ_1 and θ_2. The phase dependences of the free energy is written in the rhombohedral case as,

$$F(\theta_1) = \frac{|G|}{3} u^6 \cos(6\theta_1 + \theta_G) \tag{7}$$

This takes a minimum at $6\theta_1 = (2n + 1)\pi - \theta_G$ with the integer n. The phase θ_1 depends on the parameter θ_G. Therefore, the structural distortion shows a sine-wave modulation like an incommensurate structure. The phase will depend on temperature. The space group of this rhombohedral structure is $R3$.

In the hexagonal case, the phase dependence becomes,

$$\begin{aligned} F(\theta_1, \theta_2) &= \frac{|G|}{24} u^6 (\cos(6\theta_1 + \theta_G) + \cos(6\theta_2 + \theta_G) \\ &\quad + \frac{|H|}{24} u^6 \cos(3(\theta_1 + \theta_2) + \theta_H) + \frac{I}{24} u^6 \cos 3(\theta_1 - \theta_2) \\ &= \frac{|G|}{12} u^6 \cos(\theta_a + \theta_G) \cos \theta_s + \frac{|H|}{24} u^6 \cos(\theta_a + \theta_H) \\ &\quad + \frac{I}{24} u^6 \cos \theta_s, \end{aligned} \tag{8}$$

$$\tag{9}$$

where, $\theta_a = 3(\theta_1 + \theta_2)$, and $\theta_s = 3(\theta_1 - \theta_2)$. The θ_s depends on the sign of I. For $I > 0$, $\theta_s = (2n + 1)\pi$. Then, the space group becomes $P312$. For $I < 0$, $\theta_s = 2n\pi$, and its space group is $P\bar{6}$. The remaining θ_a can be obtained from $\partial F / \partial \theta_a = 0$, and depends on the parameters, θ_G and θ_H. Therefore, in the hexagonal case, both phases of θ_1 and θ_2 will show temperature dependence. The obtained three structures are summarized in Table 1.

These structures depend on the phases θ_1 and θ_2. Therefore, a definite structure cannot be drawn. Instead, we can describe a structure as a linear combination of two structures. For the rhombohedral $R3$ structure, we define $R3$:c with $\theta_1 = 0$ and $R3$:s with $\theta_1 = \pi/2$. Then, the structure can be made schematically by $(R3 : c) \cos \theta_1 + (R3 : s) \sin \theta_1$. Similarly, we define $P\bar{6}$:c with $(\theta_1, \theta_2) = (0, 0)$, $P\bar{6}$:s with $(\pi/2, \pi/2)$, $P312$:c with $(0, \pi)$, and $P312$:s with $(\pi/2, 3\pi/2)$ for the hexagonal structures. The $R3$:c structure has the c-type structure in c-plane as shown in Fig. S1(b). The $R3$:s structure has the s-type

2

structure as shown in Fig. S1(a). The stacking along the c-direction obeys the periodicity of the Rhombohedral lattice.

In the main text, the $R3$:s structure is introduced as an example, and is shown in Fig. 5. In the $P\bar{6}$:c structure, the c-type structure stacks along the c-direction as $+2$, -1, and -1 displacement. In the $P\bar{6}$:s structure, the s-type structure stacks as $+2$, -1, and -1. In the $P312$:c structure, the s-type structure stacks as 0, $+1$, and -1. Finally, in the $P312$:s structure, the c-type structure stacks as 0, $+1$, and -1.

For all cases, we can write the free energy as following.

$$F = \frac{A(T - T_s)}{2}u^2 + \frac{b}{4}u^4 + \frac{c}{6}u^6. \tag{10}$$

Below T_s, the order parameter can be obtained from $dF/du = 0$. The solution without $u = 0$ is,

$$u^2 = \frac{-b + \sqrt{b^2 + 4A(T_s - T)c}}{2c}. \tag{11}$$

Here, we do not describe the detailed free energy for A_1 or E. In these cases, the free energy has a third-order term, like u^3, since $3\mathbf{q}_1$ is a reciprocal lattice vector and there is no operation to convert u to $-u$. Therefore, from the Landau theory, the transition will be the first-order. This is inconsistent with the experimental result, which is second-order transition. From this point of view, the order-parameter will belong to A_2.
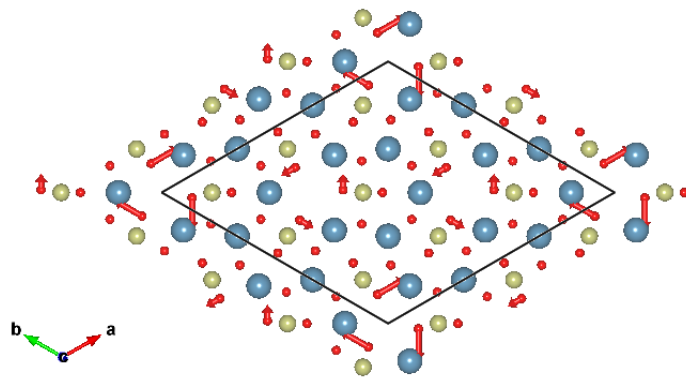
(a)
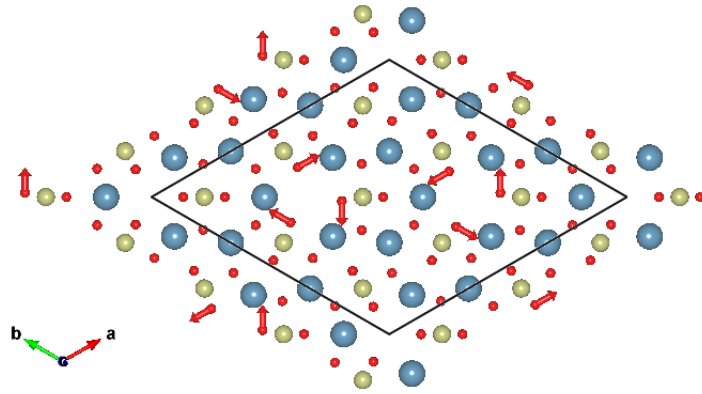
(b)

Figure S1: The possible structural changes by A_2 order-parameter, where only O(1) displacement is shown. (a) An s-type distortion. (b) A c-type distortion.